

Narrow Spectral Linewidth Full-Band Wavelength Tunable Lasers for Digital Coherent Communication Systems

Tsutomu ISHIKAWA*, Hirokazu TANAKA, Masao SHIBATA, Mikio TAJIMA, Yoshiki OKA and Toshimitsu KANEKO

Full-band wavelength tunable lasers with high optical output power and narrow spectral linewidth have been required for digital coherent communication systems. Sumitomo Electric Industries, Ltd. manufactures integrable tunable laser assemblies (ITLAs) using chirped-sampled-grating distributed-reflector laser diodes (CSG-DR-LDs) as full-band wavelength tunable laser suitable for high optical output power operation. The authors optimized multi quantum well (MQW) active layers in the CSG-DR-LD, and achieved high optical output power of over +16dBm and narrow spectral linewidth below 200 kHz. These characteristics make the lasers promising for 100 Gbit/s digital coherent communication systems.

Keywords: tunable laser, optical power, line width, ITLA, digital coherent

1. Introduction

In order to catch up with the rapid increase in data traffic, digital coherent technology using coherent detection and digital signal processing has been developed for optical fiber communication systems, in addition to dense wavelength division multiplexing (DWDM) technology⁽¹⁾⁻⁽³⁾. In comparison with conventional on-off keying modulation, various modulation formats using coherent detection, for example dual-polarization quadrature phase-shift keying (DP-QPSK) or dual-polarization 16 quadrature amplitude modulation (DP-16QAM), improve frequency band efficiency and promise over 100 Gbit/s transmission per WDM channel. These communication systems require full-band wavelength tunable lasers with high optical power and narrow spectral linewidth as a light source in the transmitter and a local oscillator in the receiver.

Sumitomo Electric Industries, Ltd. has developed chirped-sampled-grating distributed-reflector laser diodes (CSG-DR-LDs) as full-band wavelength tunable lasers with high optical output power of over +16 dBm⁽⁴⁾⁻⁽⁶⁾, and manufactures integrable tunable laser assemblies (ITLAs) equipped with special control circuits, which are compliant with the OIF-MSA^{s1} standard⁽⁷⁾. In this report, we optimized multi quantum well (MQW) active layers in the CSG-DR-LD, have achieved high optical output power of over +16 dBm, and created narrow spectral linewidth below 200 kHz as a promising light source for 100 Gbit/s digital coherent communication systems.

2. Device Structure and Mechanism

Figure 1 shows the schematic structure of a CSG-DR-LD. It consists of three sections: a semiconductor optical amplifier (SOA), sampled-grating distributed feedback (SG-DFB), and chirped-sampled-grating distributed Bragg

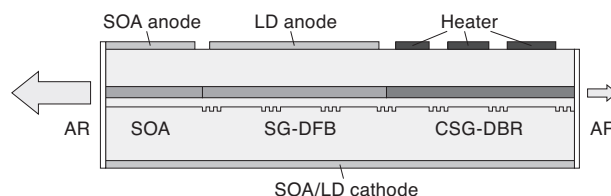


Fig. 1. Schematic structure of CSG-DR-LD

reflector (CSG-DBR) from the front facet toward the rear facet. Both facets are coated with anti-reflection (AR) film. The SG-DFB section and the CSG-DBR section constitute the laser cavity. The basic configuration of the laser cavity is the same as the distributed-reflector (DR) laser, which has a passive distributed Bragg reflector (DBR) integrated on the rear side of an active distributed feedback (DFB)⁽⁸⁾. This configuration is suitable for high optical output power, because it can efficiently emit the lasing light from the front facet, even if the both facets are AR coated. Furthermore, by introducing proper phase shift in the diffraction gratings, it does not need the phase control electrode used in the DBR-type tunable laser configuration⁽⁹⁾.

The SG-DFB section provides gain for lasing by current injection from an LD anode. Due to sampled gratings (SGs) being arranged in the same interval in the SG-DFB section, periodic peaks appear in the gain spectrum due to the interference of reflected light from each SG. In the CSG-DBR section, the intervals between adjacent SGs are slightly different from each other. These chirped SGs result in periodic peaks in the reflection spectrum whose envelope shows a moderate swell. This shape of the envelope works as a band-pass filter. Wavelengths of the periodic reflection peaks and the filter wavelength (peak wavelength of the envelope) are thermally controlled by three heaters integrated on the top of the CSG-DBR section. The SOA section controls output power from the front facet, and

also works as a shutter of unstable light output during the start-up routine or wavelength switching routine.

Figure 2 shows the calculated reflection spectra for the CSG-DBR. Each spectrum corresponds to the various temperature settings of the three heaters so that the filter wavelength is tuned throughout a wide wavelength range. In each graph, we show the temperature difference between the three heaters as T . When all the three heaters have the same temperature, i.e. $T = 0$ K, the filter wavelength of CSG-DBR is the same as the Bragg wavelength of the diffraction gratings. If the temperature of each heater is different from each other, the filter wavelength is changed from the Bragg wavelength. For example, when the temperature of each heater gradually increases in order, as the interval of the SGs becomes longer, the filter wavelength becomes longer. On the other hand, the filter wavelength becomes shorter, if the temperature of each heater gradually decreases in order, as the interval of SGs becomes longer. The amount of the filter wavelength change is proportional to the temperature difference between each heater. We defined the sign of T as subtracting heater temperature on the SGs with the shortest interval from that on SGs with the longest interval. Therefore, when T is positive, the filter wavelength becomes longer. On the other hand, when T is negative, the filter wavelength becomes shorter. The heater temperature on the SGs with middle interval is set to the average temperature of the other two heaters. As the tuning mechanism of the filter wavelength for the CSG-DBR is based on a small difference in the interval between each SG, we can widely tune the filter wavelength by a relatively small temperature difference. According to the calculation, the temperature difference of about $|T| = 15$ K leads to the full-band wavelength range.

The whole shape of the reflection spectrum for the CSG-DBR shifts in proportion to the whole temperature of the CSG-DBR section. So, we can control the wavelength of periodic reflection peaks independently of the filter wavelength, by changing the temperature of all heaters while keeping the temperature difference of each heater constant. In other words, the wavelength of the periodic reflection peaks is controlled by the average temperature of the three heaters, while the filter wavelength is controlled by the temperature difference of each heater.

The lasing mode of the CSG-DR-LD is determined by using the Vernier effect, caused by periodic gain peaks of the SG-DFB and periodic reflection peaks of the CSG-DBR. The period of gain peaks for SG-DFB and that of the reflection peaks for the CSG-DBR are slightly different from each other, and therefore, one of the gain peaks of the SG-DFB that coincides with one of the reflection peaks of the CSG-DBR can be selected as the lasing mode. As the wavelength of the periodic reflection peaks of the CSG-DBR shifts in proportion to the average temperature of the three heaters, we can arbitrarily select the lasing mode from any of the gain peaks for SG-DFB.

However, in the lasing mode selection, by using the Vernier effect, another gain peak may coincide with one of the reflection peaks for the CSG-DBR, which is away from the target lasing mode by wavelength interval determined by the difference between the two periods of gain peaks for SG-DFB and reflection peaks for the CSG-DBR.

These unnecessary modes, which we call recursive modes, have to be restrained for stable single mode operation. The filter function for the CSG-DBR coarsely restricts the lasing

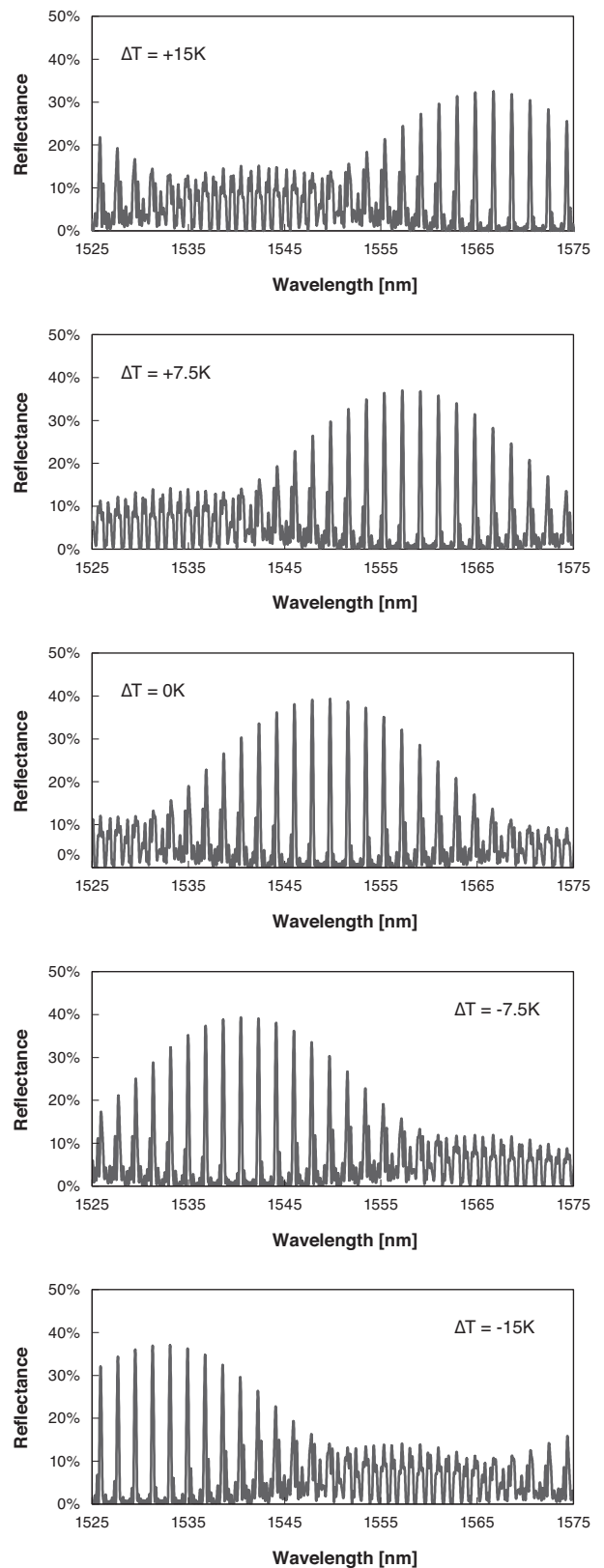


Fig. 2. Calculated reflection spectra of CSG-DBR

wavelength around the filter wavelength, and restrains the recursive modes from lasing. To be concrete, the filter wavelength is set to the target lasing mode by controlling the temperature difference of the three heaters, while at the same time selecting the lasing mode by controlling the average temperature of the three heaters.

Furthermore, the whole spectrum of the gain peaks for SG-DFB and that of the reflection peaks for the CSG-DBR shift in proportion to the entire chip temperature. We can tune the wavelength of the selected lasing mode by controlling the entire chip temperature with a thermoelectric cooler (TEC).

Table 1 summarizes the wavelength tuning method for the CSG-DR-LD. Three functions to determine the lasing wavelength for the CSG-DR-LD can be controlled independently of each other. They show good linearity, and are described in simple formulas, because they are based on the temperature dependence of the refractive index of semiconductors. In addition, no phase control of the laser cavity is needed, because the phase condition of the laser cavity is always matched by the phase shift structure introduced in diffraction gratings.

Table 1. Wavelength tuning method of CSG-DR-LD

Function	Control parameter
Filter wavelength tuning of CSG-DBR	Temperature difference of 3 heaters
Lasing mode selection by Vernier effect	Average temperature of 3 heaters
Continuous wavelength tuning of selected mode	Chip temperature (TEC)

3. Reduction of Linewidth Enhancement Factor

The spectral linewidth ν for semiconductor lasers is described in the following equation⁽¹⁰⁾.

$$\Delta\nu = \frac{h\nu v_g^2 g_{th} \alpha_m n_{sp}}{4\pi P} (1 + \alpha^2) \dots\dots\dots (1)$$

Here, h is the Planck constant, ν is the frequency of propagating light, v_g is the group velocity of propagating light, g_{th} is the threshold gain of lasing mode, α_m is the mirror loss of laser cavity, n_{sp} is the spontaneous emission factor or population inversion parameter, P is the total optical power from the laser cavity. α is one of the main factors which broaden the spectral linewidth of semiconductor lasers, and called linewidth enhancement factor or α -parameter. It represents the phenomena where carrier fluctuation induced by the fluctuation of the optical intensity in the laser cavity causes an increase in phase noise via refractive index change of the optical waveguide. The linewidth enhancement factor α is defined as the ratio of the refractive index change dn_r/dN relative to the gain change dg/dN under the carrier density change, and described in the following equation.

$$\alpha = - \frac{4\pi}{\lambda} \frac{dn_r/dN}{dg/dN} \dots\dots\dots (2)$$

Here, λ is the wavelength of the propagating light, N is the carrier density, n_r is the equivalent refractive index of the propagating light, g is the modal gain of the propagating light. The gain change ratio relative to the carrier density change dg/dN is also called differential gain.

As shown in **equation (2)**, the larger differential gain dg/dN gives a smaller α -parameter. Particularly for MQW active layers in the CSG-DR-LD, it is important that the injected carriers from the LD current efficiently generate optical gain in the quantum well layers. Furthermore, the overflow carriers into the barrier layers or separate confinement heterostructure (SCH) layers included in the MQW active layers drastically increase the α -parameter, because they cause a refractive index change by plasma effect although they generate no gain. Therefore, we attempted to restrain the overflow carriers into barrier layers or SCH layers by optimizing the MQW structure to have a higher energy barrier in order to confine the carriers in the quantum wells.

At first, we fabricated various Fabry-Perot laser diodes (FP-LDs) having MQW active layers with a different energy barrier height for quantum wells in order to compare their α -parameter. The laser cavity of the FP-LDs was designed to have a larger threshold gain than that of the CSG-DR-LD. We measured the amplified spontaneous emission (ASE) spectra while changing the injection current in the range of well below the threshold current for FP-LDs. We evaluated a refractive index change from the wavelength change of each Fabry-Perot mode appearing in the ASE spectrum at each injection current. The gain change was also evaluated from each ASE spectrum with the Hakki-Paoli method⁽¹¹⁾. Then, the α -parameter was evaluated with the given refractive index change and gain change. **Figure 3** shows the evaluated α -parameter for FP-LDs with MQW active layers previously used in the CSG-DR-LD and the high barrier MQW active layers adopted in this work. Here, the injection current of each FP-LD is adjusted so that the gain of the FP-LD matches the threshold gain of the CSG-

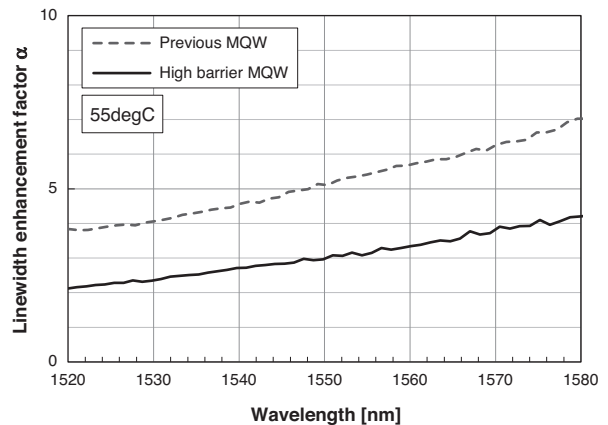


Fig. 3. Measured linewidth enhancement factor

DR-LD. The high energy barrier for the quantum wells resulted in 60% reduction of the α -parameter relative to the previously used MQW active layers. The difference in energy barrier height between the two MQWs is 50 meV at conduction band. It is expected to result in 50% reduction of the spectral linewidth of the CSG-DR-LD by adopting this high barrier MQW.

4. Lasing Characteristics and Effective Linewidth

Next, we fabricated the CSG-DR-LDs with the high barrier MQW active layers. We tuned the lasing wavelength of the CSG-DR-LD to the 50 GHz channel spacing ITU-T^{*2} grids by setting the temperature of the three heaters and TEC in the way described in section 2. The injection current of the LD anode is set to 175 mA for all channels. **Figure 4** shows the fiber output power and SOA current. High optical output power levels of over +16.5 dBm were achieved with SOA currents below 200 mA. **Figure 5** shows the side mode suppression ratio (SMSR). The stable single mode operation with SMSRs of over 45 dB is confirmed as extended to the range of 122 channels with channel spacing

of 50 GHz (a wavelength range of 1523.75-1572.05 nm). **Figure 6** shows the effective linewidth measured with an etalon discriminator⁽¹²⁾. Narrow linewidth levels below 200 kHz were achieved and extended to the range of 96 channels.

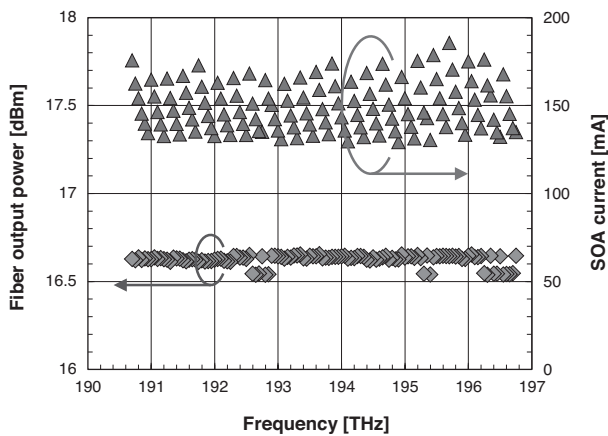


Fig. 4. Optical output power and SOA current

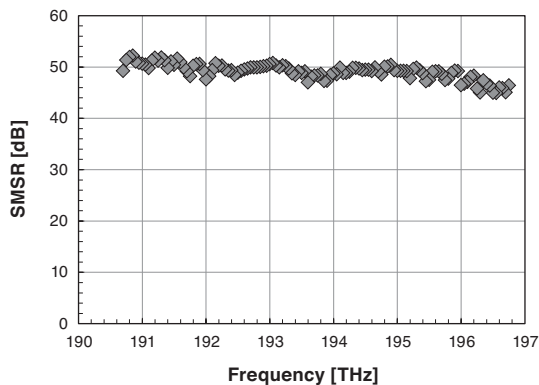


Fig. 5. Side mode suppression ratio

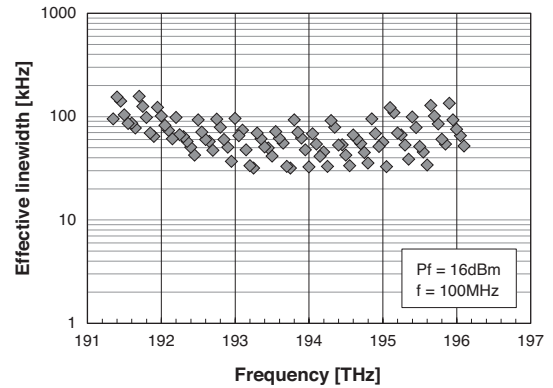


Fig. 6. Effective linewidth

5. Conclusion

We optimized MQW active layers in the CSG-DR-LD to reduce the linewidth enhancement factor, achieved high optical output power of over +16 dBm and narrow spectral linewidth below 200 kHz. It is promising for 100 Gbit/s digital coherent communication systems.

Technical Terms

- *1 OIF-MSA: Optical Internetworking Forum Multi Source Agreement
- *2 ITU-T: International Telecommunication Union Telecommunication Standardization Sector

References

- (1) S. Tsukamoto, D.-S. Ly-Gagnon, K. Katoh, and K. Kikuchi, "Coherent demodulation of 40-Gbit/s polarization-multiplexed QPSK signals with 16-GHz spacing after 200-km transmission," presented at the Optical Fiber Communications Conference (OFC), Anaheim, CA, Mar. 2005, Paper PDP29.
- (2) S. Oda, T. Tanimura, T. Hoshida, C. Ohshima, H. Nakashima, Z. Tao, and J. C. Rasmussen, "112 Gb/s DP-QPSK transmission using a novel nonlinear compensator in digital coherent receiver," presented at the Optical Fiber Communications Conference (OFC), San Diego, CA, Mar. 2009, Paper OThR6.
- (3) A. Sano, H. Masuda, T. Kobayashi, M. Fujiwara, K. Horikoshi, E. Yoshida, Y. Miyamoto, M. Matsui, M. Mizoguchi, H. Yamazaki, Y. Sakamaki, and H. Ishii, "69.1-Tb/s (432 x 171-Gb/s) C- and extended L-band transmission over 240 Km using PDM-16-QAM modulation and digital coherent detection," presented at the Optical Fiber Communications Conference (OFC), San Diego, CA, Mar. 2010, Paper PDKPB7.
- (4) T. Ishikawa, T. Machida, H. Tanaka, Y. Oka, H. Shoji, T. Fujii, and S. Ogita, "A novel high output power full-band wavelength tunable laser with monolithically integrated single stripe structure," Proc. 33rd European Conf. on Opt. Commun., no. PD2.4, Berlin, Germany, Sept. 2007.
- (5) H. Tanaka, T. Ishikawa, T. Machida, Y. Yamauchi, Y. Oka, T. Fujii, and H. Shoji, "High power and full-band wavelength tunable laser module," Proc. of 2008 IEICE General Conf., no. C-4-20, p. 303, Mar. 2008.
- (6) T. Ishikawa, T. Machida, H. Tanaka, T. Kaneko, Y. Oka, T. Tajima, H. Shoji, and T. Fujii, "High-power single-stripe full-band tunable laser using tunable reflector with wavelength-filter function," IEICE Technical Report, vol. 108, no. 114, LQE2008-30, pp. 51-56, Jun. 2008.
- (7) M. Okamoto, E. Banno, Y. Kondoh, T. Matsumura, M. Ono, and H. Kawamura, "High optical power full-band ITLA," Proc. of 2010 IEICE General Conf., no. C-3-65, p. 238, Mar. 2010.
- (8) J.-I. Shim, K. Komori, S. Arai, I. Arima, Y. Suematsu, and R. Somchai, "Lasing characteristics of 1.5 μm GaInAsP-InP SCH-BIG-DR lasers," IEEE J. Quantum Electron., vol. QE-27, no. 6, pp. 1736-1745, 1991.
- (9) V. Jayaraman, Z.-M. Chuang, and L. A. Coldren, "Theory, design, and performance of extended tuning range semiconductor lasers with sampled gratings," IEEE J. Quantum Electron., vol. QE-29, no. 6, pp. 1824-1834, 1993.
- (10) C. H. Henry, "Theory of the linewidth of semiconductor lasers," IEEE J. Quantum Electron., vol. QE-18, no. 2, pp. 259-264, 1982.
- (11) B. W. Hakki, and T. L. Paoli, "CW degradation at 300K of GaAs double-heterostructure junction laser II. Electronic gain," J. Appl. Phys., vol. 44, pp. 4113-4119, 1973.
- (12) T. Kaneko, Y. Yamauchi, H. Tanaka, T. Machida, T. Ishikawa, T. Fujii, and H. Shoji, "High-power and low phase noise full-band tunable LD for coherent applications," presented at the Optical Fiber Communications Conference (OFC), San Diego, CA, Mar. 2010, Paper OWU7.

Contributors (The lead author is indicated by an asterisk (*).)

T. ISHIKAWA *

- Transmission Devices R&D Laboratories



H. TANAKA

- Sumitomo Electric Device Innovation Ltd.



M. SHIBATA

- Sumitomo Electric Device Innovation Ltd.



M. TAJIMA

- Analysis Technology Research Center



Y. OKA

- Sumitomo Electric Device Innovation Ltd.



T. KANEKO

- Transmission Devices R&D Laboratories

